This work was carried out in whole or in part within the framework of the NOMATEN Center of Excellence, supported from the European Union Horizon 2020 research and innovation programme (Grant Agreement No. 857470), the European Regional Development Fund via the Foundation for Polish Science International Research Agenda PLUS programme (Grant No. MAB PLUS/2018/8), *and the initiative of the Ministry of Science and Higher Education 'Support for the activities of Centers of Excellence established in Poland under the Horizon 2020 program' under agreement No. MEiN/2023/DIR/3795.*

This is a copy of the publication which appeared in J Biomed Mater Res.2024;112:e35404, published in March 2024.

DOI: 10.1002/jbm.b.35404

Received: 25 September 2023 | Revised: 12 February 2024 | Accepted: 13 March 2024

DOI: 10.1002/jbm.b.35404

RESEARCH ARTICLE

Society For Biomaterials | WILEY

Albumin suppresses oxidation of Ti—Nb alloy in the simulated inflammatory environment

Agata Sotniczuk[1,2] | Damian Kalita[1] | Witold Chromiński[1,2] | Magdalena Matczuk[3] | Marcin Pisarek[4] | Halina Garbacz[2]

[1]NOMATEN Centre of Excellence, National Centre for Nuclear Research, Otwock, Poland

[2]Faculty of Materials Science and Engineering, Warsaw University of Technology, Warsaw, Poland

[3]Chair of Analytical Chemistry, Faculty of Chemistry, Warsaw University of Technology, Warsaw, Poland

[4]Laboratory of Surface Analysis, Institute of Physical Chemistry, Polish Academy of Sciences, Warsaw, Poland

Correspondence
Agata Sotniczuk, NOMATEN Centre of Excellence, National Centre for Nuclear Research, A. Sołtana 7, 05-400 Otwock-Swierk, Poland.
Email: agata.sotniczuk@ncbj.gov.pl; agata.sotniczuk@pw.edu.pl

Funding information
National Science Centre, Poland, Grant/Award Number: PRELUDIUM 15 [2018/29/N/ST8/02306]; European Union Horizon 2020, Grant/Award Number: 857470; European Regional Development Fund; Foundation for Polish Science International Research Agenda PLUS program, Grant/Award Number: MAB PLUS/2018/8; Ministry of Science and Higher Education 'Support for the activities of Centers of Excellence established in Poland under the Horizon 2020 program', Grant/Award Number: MEiN/2023/DIR/3795

Abstract

Literature data has shown that reactive oxygen species (ROS), generated by immune cells during post-operative inflammation, could induce corrosion of standard Ti-based biomaterials. For Ti—6Al—4V alloy, this process can be further accelerated by the presence of albumin. However, this phenomenon remains unexplored for Ti β-phase materials, such as Ti—Nb alloys. These alloys are attractive due to their relatively low elastic modulus value. This study aims to address the question of how albumin influences the corrosion resistance of Ti—Nb alloy under simulated inflammation. Electrochemical and ion release tests have revealed that albumin significantly enhances corrosion resistance over both short (2 and 24 h) and long (2 weeks) exposure periods. Furthermore, post-immersion XPS and cross-section TEM analysis have demonstrated that prolonged exposure to an albumin-rich inflammatory solution results in the complete coverage of the Ti—Nb surface by a protein layer. Moreover, TEM studies revealed that H_2O_2-induced oxidation and further formation of a defective oxide film were suppressed in the solution enriched with albumin. Overall results indicate that contrary to Ti—6Al—4V, the addition of albumin to the PBS + H_2O_2 solution is not necessary to simulate the harsh inflammatory conditions as could possibly be found in the vicinity of a Ti—Nb implant.

KEYWORDS
albumin adsorption, implants, inflammation, nanometric oxide films, reactive oxygen species, titanium β-phase alloys

1 | INTRODUCTION

Corrosion behavior of biomedical materials devoted to permanent implants is typically verified in solutions such as Hank's solution,[1] Ringer's solution[2] or phosphate-buffered saline (PBS).[3] However, literature data have shown that currently used metallic biomaterials could experience corrosion in the human body despite the high corrosion resistance confirmed by laboratory in vitro tests performed in solutions mentioned above.[4–7] Corrosion of implants observed in vivo could be related to the release of reactive oxygen species (ROS) such as hydrogen peroxide (H_2O_2) by human immunological cells during post-operative inflammatory reaction.[4,8,9] To date, accelerated corrosion induced by the presence of H_2O_2 was observed for titanium-based biomaterials such as commercially pure Ti: CP—Ti (α phase)[10–12] and Ti—6Al—4V (α + β phase) alloy,[13–15] which are currently exploited in long-lasting implantology. In vitro corrosion studies revealed that

the addition of H_2O_2 to biological solutions resulted in the decrease of the passive layer resistance,[12] surface roughening,[16] discoloration,[14] and rebuilding of the spontaneously formed oxide film into a thicker and more defective during long immersion periods.[17,18]

It has to be mentioned that immunological cells, which are responsible for ROS release, have limited ability to directly interact with metallic surfaces.[19] Their activity is regulated by blood proteins (such as albumin), which immediately adsorb on the implanted metallic surface creating blood-based transient provisional matrix.[19] To date, the corrosion resistance under the simultaneous presence of inflammatory products (H_2O_2) and albumin has been verified for the Ti—6Al—4V alloy.[20–25]

The deleterious effect of albumin on the corrosion resistance of Ti—6Al—4V under simulated inflammatory conditions was confirmed by both electrochemical (potentiodynamic polarization[20] and EIS[22,25]) and spectrometric (ICP-MS[20,23]) techniques. One hypothesis claims that this phenomenon is associated with the suppression of the cathodic reaction by albumin, which shifts OCP to more negative values and thereby accelerates Ti—6Al—4V degradation induced by H_2O_2.[20] Conclusions derived from corrosion measurements were supported by the results of further surface analysis performed after prolong Ti—6Al—4V immersion in the biological solutions.[20,23] XPS studies indicate that the simultaneous presence of albumin and H_2O_2 promotes both complexation reactions between Ti and H_2O_2 and between Al and albumin. Moreover, XPS analysis revealed that the oxide layer formed after 2 weeks of Ti—6Al—4V exposure in PBS + H_2O_2 + albumin did not contain V, which suggest the preferential dissolution of the β phase.[23] This confirms findings derived from previously performed SEM observations, in which it was demonstrated that the privileged degradation of the β phase, is intensified by the presence of albumin.[20]

Preferential dissolution of the β phase observed in two-phased alloy justifies the necessity to verify if the presence of albumin accelerates H_2O_2-induced corrosion in the case of single β-phase Ti alloys, such as those from the Ti—Nb system, which are currently widely studied owing to their reduced stiffness combined with high biocompatibility.[26–29] Solution-treated binary Ti—Nb alloys with Nb addition in the range of 40–45 wt% demonstrate a low elastic modulus (between 60 and 65 GPa), which is much closer value to the stiffness of human cortical bone (10–30 GPa) compared to standard Ti-based biomaterials (100–120 GPa).[30] Advantages of β-phase Ti—Nb alloys also include optimized manufacturing procedure, which allows obtaining relatively large quantities of semi-finished products needed to fabricate implantable devices. In addition to traditional thermomechanical fabrication procedures, literature data demonstrate possibility to process β-phase Ti—Nb alloy by additive manufacturing techniques with the possibility to fully control its microstructure and final shape.[29] High corrosion resistance of biomedical β-phase Ti—Nb alloys, such as Ti—45Nb alloy, has been confirmed in non-organic biological fluids such as Ringer's[31] solution, physiological saline[32] or artificial saliva.[33] To date, the inflammatory-induced corrosion of Ti—45Nb alloy was evaluated only based on tests performed in PBS + H_2O_2 fluid.[30,34] Therefore, the aim of this study was to provide insight into the effect of albumin on the corrosion resistance of fully β-phase Ti—45Nb alloy in the H_2O_2-enriched fluid that simulates the conditions created by the immune cells. This study offers the first step to verify whether H_2O_2 sufficiently simulates the aggressiveness of the post-operative inflammatory environment or if the addition of proteins is necessary to truly reflect these conditions.

2 | MATERIALS AND METHODS

Commercially available Ti—45Nb, supplied by WOLFTEN Company was used as the tested material. The composition of the alloy was as follows (max wt.%): 0.019% C, 0.006% N, 0.058% O, 0.001% H, and 44.57% Nb with the balance of Ti. The supplied Ti—45Nb alloy was subjected to heat-treatment in order to obtain a homogenous, recrystallized microstructure fully composed of micrometric grains of the β-phase. To achieve this microstructure, Ti—45Nb was annealed at 1000°C for 2 h and subsequently fast-cooled by quenching in water. During annealing, Ti—45Nb was placed in glass capsule filled with argon. The capsule was broken-immediately during the quenching procedure. The microstructure of the alloy was composed from equiaxed grains of the β-phase with the following average size: Avg (d_2) = 79 μm, SD (d_2) = 49 μm as detailed in Ref. 34. Samples devoted to corrosion experiments were ground with SiC abrasive paper (gradation: #600, #1200, #2400) and polished with a silica suspension (a Struers, OP-S, gradation = 0.04 μm) from the sites exposed to the corrosion solutions. Prepared samples were ultrasonically cleaned with isopropanol, dried in compressed air and stored in a desiccator for 2 h before each test. The same time gap between polishing and corrosion tests was respected for all samples, considering the possibility of titanium oxide layer evolution during prolong exposure to air.[35]

Corrosion evaluation included both electrochemical and ion-release measurements. Corrosion tests were carried out in two solutions that simulate post-operative inflammatory conditions: (i) PBS + 0.1% H_2O_2 and (ii) PBS + 0.1% H_2O_2 + 4% albumin. Pure PBS solution was made from PBS tablets (Sigma Aldrich) dissolved in the deionized water. PBS + 0.1% H_2O_2 (PBS + 30 mM H_2O_2) was prepared by adding 1 mL of H_2O_2 (30 wt % in H_2O, Sigma Aldrich) to 300 mL of PBS solution. In order to prepare PBS + 0.1% H_2O_2 + 4% albumin, PBS + 0.1% H_2O_2 was enriched with bovine serum albumin (lyophilized powder, ≥98%, Sigma Aldrich). The concentration of albumin (BSA) was similar to that in human blood.[22,23] For all experiments, solutions were made directly before samples immersion, which was justified by instability of H_2O_2.

Electrochemical tests were carried out with potentiostat (a Metrohm Autolab PGSTAT 302N) coupled with a three-electrode system containing: (i) working electrode: Ti—45Nb sample, (ii) reference electrode: Ag/AgCl electrode placed in a Luggin capilary, (iii) counter electrode: graphite rod. The electrochemical cell with the three-electrode system was placed in an incubator at 37°C. The tested surface area was the same for all samples (~0.1 cm^2, adjusted by an O-Ring with a 3.5 mm inner diameter). The procedure

of electrochemical tests was as follows: (i) open circuit potential (OCP) monitoring for 2 h after immersion in the solutions, (ii) electrochemical impedance spectroscopy (EIS) analysis performed after 2 and 24 h of immersion. EIS tests were performed at OCP for frequencies from the range of 10^4 Hz to 5×10^{-3} Hz.

In addition to the electrochemical tests, the corrosion resistance of Ti—45Nb was evaluated based on the measurements of the concentration of metal ions in the solutions after prolong immersion (336 h – 2 weeks). For the immersion tests, samples were enclosed in sterile centrifuge containers containing 1 mL of PBS + H_2O_2 or PBS + H_2O_2 + BSA solution per 1 cm^2 of the sample (~4 mL of solution per 1 sample). Collected solutions were subjected to digestion with nitric acid (HNO_3, 69%, Fluka, Trace metal basis) and then diluted in water with yttrium as an internal standard (10 µg/L final concentration, Sigma–Aldrich). Before analysis, samples were filtered with 0.45 µm syringe filters. The samples containing albumin were centrifuged (12,000 rpm, 15 min) before filtration. Concentration of metal ions was evaluated using an inductively coupled plasma mass spectrometer (an ICP Triple Quadrupole Mass Spectrometer, Agilent 8900). Processing parameters were as follows: (i) flow of the gas – 1.10 L/min, (ii) type of nebulizer gases – mixture of hydrogen (8.0 mL/min) and oxygen (0.1 mL/min) (iii) RF power – 1550 W. Monitoring of the mass to charge ratio changes: 48Ti → 64Ti and 93Nb → 109Nb allowed the calculation of the total concentration of released ions.

The significance of the effect of albumin on the Ti—45Nb corrosion resistance was evaluated based one-way ANOVA analysis combined with post-hoc Tukey test ($p < 0.05$). All corrosion tests (EIS and ICP-MS) were performed for three samples ($n = 3$).

Metallic samples subjected to immersion tests were rinsed with 1 mL of deionized water, dried with compressed air, and placed into the desiccator. Then, Ti—45Nb discs were subjected to XPS measurements in order to obtain information about the surface chemical composition. XPS analysis was performed using a Microlab 350 (Thermo Electron). The applied XPS parameters were as follows: (i) exciting source – an Al Kα non-monochromatic x-ray source (with energy of 1486.6 eV and power od 300 W), (ii) analyzed surface area – 2×5 mm^2. HR-XPS spectra were deconvoluted using Gaussian/Lorentzian mixed function with the constant G/L ratio of 0.35 (±0.05). All designated binding energies were corrected using a binding energy of carbon (C1s = 285.0 eV). Additionally, XPS tests were performed for the as-polished (non-immersed) samples. This allowed assessment of the differences in surface composition induced by prolonged immersion in the simulated inflammatory environments.

Top-view XPS surface analysis was supplemented by microscopic observations of the cross-sections of the samples subjected to long-term immersion tests. To achieve this, thin lamellas were extracted from the cross-sections using FIB microscope, a Helios 5 UX DualBeam (a Thermo Fisher Scientific). To avoid significant influence of Ga ions on the structure of the thin foils, the beam accelerated voltage was progressively reduced (down to 2 kV) during the thinning procedure. In order to preserve the surface features developed during immersion, nanometric gold and platinum layers were sputtered onto the top surfaces of the samples before starting the cutting procedure. FIB lamellas were subjected to microscopic observation using TEM (a JEOL JEM 1200) with an acceleration voltage of 120 kV, which enabled obtaining a general view of Ti—Nb surfaces. Detailed observations of FIB lamellas, combined with EDS analysis, were performed with a STEM/TEM microscope (a Thermo Fischer Scientific Spectra 200) with an acceleration voltage of 200 kV. Microscopic analysis enabled to reveal the following aspects: (i) comparison of the thickness and morphological features of the oxide films formed in PBS + H_2O_2 or PBS + H_2O_2 + BSA, (ii) evaluation of the continuity and thickness of the adsorbed albumin layer.

3 | RESULTS

Electrochemical experiments began with OCP monitoring for 2 h after were immersed in the solutions simulating post-operative inflammation. It was found that the OCP value registered after 2 h of measurements was about 100 mV lower in the case of the PBS + H_2O_2 + BSA solution (Figure 1). The more negative OCP value could be associated with the suppression of the cathodic reaction (oxygen reduction) by the presence of BSA in the tested solution.[36,37]

Immediately after OCP monitoring (2 h from immersion) EIS tests were performed, and then measurements were repeated after 24 h of exposure to the PBS + H_2O_2 or PBS + H_2O_2 + BSA. The experimental results of the EIS tests are presented in Nyquist and Bode Plots (Figure 2A,B). Based on the analysis of the shape of Bode plots, frequency regions with different characteristics can be distinguished.[38] For frequencies between 10,000 and 1000 Hz (first region) phase angle values were close to 0° and the impedance value achieved c.a. 320–390 Ω*cm^2, with higher values designated from the measurements carried out in the PBS + H_2O_2 + BSA solution. In this region, impedance value was determined by the resistance of the selected fluid. For frequencies in the range of 1000–0.5 Hz, a linear relationship between log |Z| and applied frequency can be distinguished for all samples. In this region, the phase angles achieved their minimum values (approx. −80° for all samples) which is typical for capacitive behavior.[38] For the lowest frequencies (lower than 0.1 and 0.05 Hz for Ti—45Nb tested in PBS + H_2O_2 and PBS + H_2O_2 + BSA, respectively); the electrochemical response corresponds mostly to the resistance of the oxide layer under particular conditions. Based on the log |Z| values, it can be concluded that for both immersion times (2 and 24 h), the oxide layer resistance achieved significantly greater values in the PBS + H_2O_2 + BSA solution. Taking into account the presence of single semi-circles visible in the Nyquist plots, as well as the shape of the phase angle part of the Bode Spectra, a single-time constant electrochemical circuit with the constant phase element, CPE (Randles-CPE), was selected to designate the values of electrochemical parameters from the experimental EIS results (Figure 2A,B). The corrosion resistance was assessed based on the comparison of the values of the oxide layer resistance, R_{ox} (Figure 2C, Table 1). It was found that the presence of albumin in the PBS + H_2O_2 solution

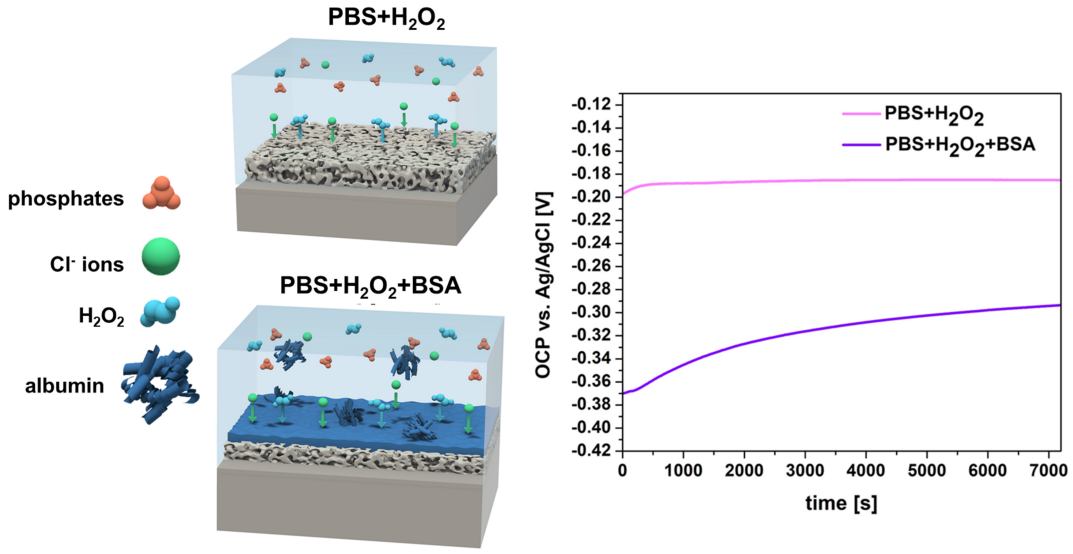

FIGURE 1 OCP monitoring during the first 2 h after samples immersion in tested solution.

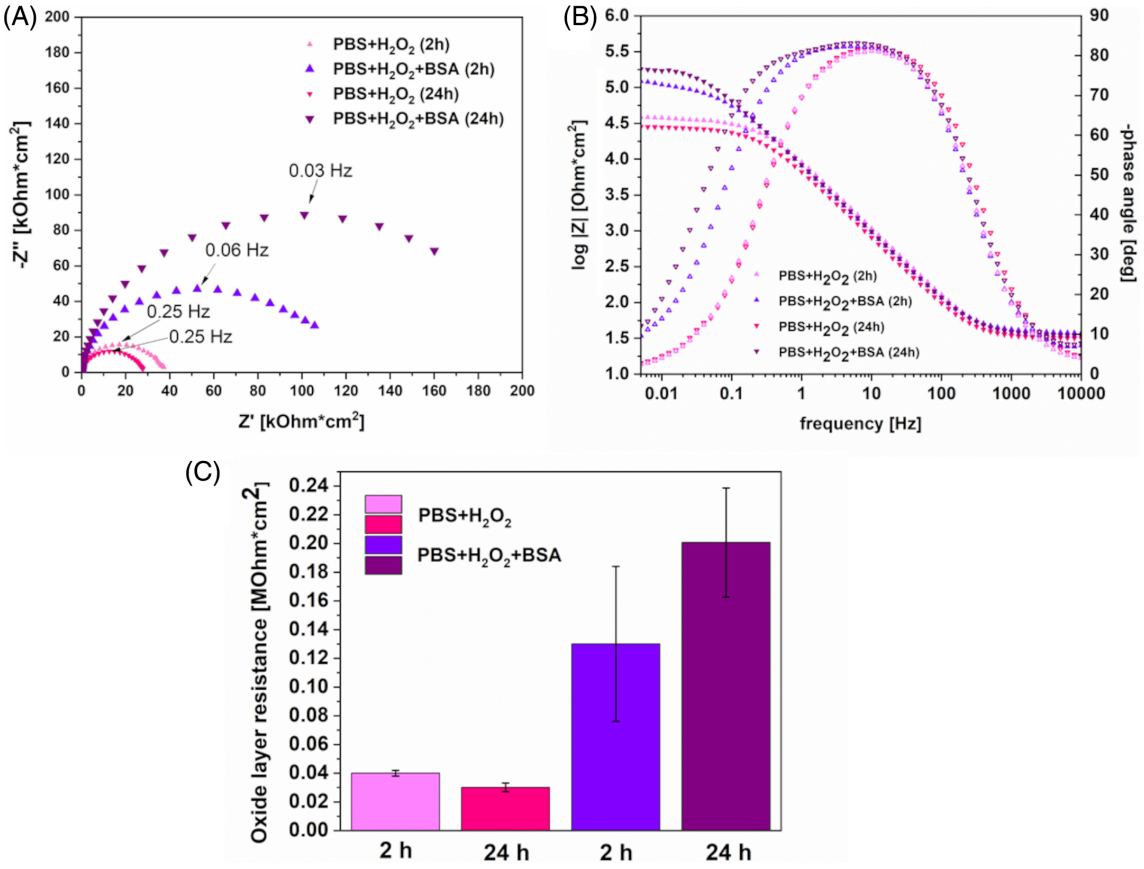

FIGURE 2 EIS data: (A–B) Nyquist and Bode Plots, respectively, illustrating results recorded after 2 and 24 h of samples exposure in the solutions that simulate post-operative inflammatory conditions, (C) oxide layer resistance values calculated from experimental EIS data.

strongly increased the corrosion resistance of Ti—Nb (Figure 2C, Table 1). Beneficial influence of albumin was found in case of shorter (2 h) as well as after longer (24 h) times of surface exposure to the simulated inflammatory fluids. The average values of R_{ox}, designated from the results of EIS tests performed in PBS + H_2O_2 + BSA, was for one order of magnitude greater compared to those calculated for PBS + H_2O_2 solution (Table 1). Difference between R_{ox} values was found to be statistically significant ($p < 0.05$). Increasing immersion

TABLE 1 Corrosion parameters designated from EIS data: R_e – resistance of electrolyte, Q and *n* – parameters of Constant Phase element, R_{ox} – oxide layer resistance, χ^2_{max} – maximum χ^2 value related to the fitting procedure (Maximum errors related to the fitting of particular parameters are included in brackets).

	Time (h)	Re (Ω*cm^2)	Q ($\times10^{-5}$ Ω^{-1} cm^{-2} s^n)	*n*	R_{ox} (MΩ*cm^2)	χ^2 max
PBS + H_2O_2	2	320 ± 17 (0.79%)	2.43 ± 0.87 (0.87%)	0.94 (0.19%)	0.04 ± 0.002 (0.79%)	0.037
	24	301 ± 18 (0.75%)	2.54 ± 0.16 (0.87%)	0.94 (0.20%)	0.03 ± 0.003 (0.75%)	0.034
PBS + H_2O_2 + BSA	2	389 ± 31 (0.88%)	2.08 ± 0.31 (0.72%)	0.94 (0.18%)	0.13 ± 0.054 (1.16%)	0.039
	24	349 ± 7 (0.79%)	2.69 ± 0.82 (0.82%)	0.92 (0.54%)	0.20 ± 0.038 (1.13%)	0.028

TABLE 2 Capacitance values derived from EIS data based on (i) approach presented by Hsu and Mansweld (H-L)[40] and (ii) Power-Law (P-L) formula.[44] Oxide layer thicknesses designated from the capacitance values.

	Time (h)	Q ($\times10^{-5}$ Ω^{-1} cm^{-2} s^n)	C_{eff} (H-L) ($\times10^{-5}$ F cm^{-2})	d_{eff} (H-L) (nm)	C_{max} (P-L) ($\times10^{-5}$ F cm^{-2})	d_{max} (P-L) (nm)
PBS + H_2O_2	2	2.43 ± 0.87	2.42 ± 0.76	2.4 ± 0.62	1.25 ± 0.36	4.7 ± 1.16
	24	2.54 ± 0.16	2.45 ± 0.10	2.2 ± 0.09	1.21 ± 0.24	4.7 ± 1.04
PBS + H_2O_2 + BSA	2	2.08 ± 0.31	2.21 ± 0.24	2.4 ± 0.29	1.12 ± 0.17	5.0 ± 0.81
	24	2.69 ± 0.82	3.04 ± 0.87	1.88 ± 0.45	1.37 ± 0.35	4.2 ± 0.96

time from 2 to 24 h did not influence the corrosion resistance of Ti—Nb in both solutions. Considering the standard deviation values (calculated based on the results obtained for three independent samples for each solution) differences in the R_{ox} values designated from EIS tests performed after 2 and 24 h were found to be non-significant. Apart from the R_{ox} value, the fitting procedure allowed to derive the values of CPE element (Q and *n* – Table 1) that were further exploited to calculate the interfacial capacitance value (C_{eff}). Literature studies present different approaches to designate C_{eff} value from calculated CPE parameters.[39] The expression presented by Hsu and Mansweld[40] has been used previously to calculate the capacitance of the oxide films formed on titanium surface.[41] This formula considered the values of both CPE parameters (Q and *n*) as well as designated values of R_{ox} (1). Capacitance values derived based on (1) equation were in the range of 2–3 $\times$ 10^{-5} F cm^{-2} (Table 2). Obtained C_{eff} values were further exploited to calculate the thickness of the oxide layers (d_{eff}) formed on particular surfaces (2). As can be noticed, for all samples average d_{eff} values did not exceed 2.5 nm (Table 2) which is much lower value compared to the titanium oxide layer thickness assessed based on the results of spectroscopy methods such as AES or XPS.[42,43] Therefore, the further step was to designate the C_{eff} value based on the Power-Law approach (3)–(5).[39] When the value of the *n* parameter is close to unity (like in our case *n* = 0.93–0.94) C_{eff} should be close to the value of C_{max} (5).[44] Therefore, d_{max} should be close to d_{eff} which is the thickness of the oxide layer. This approach has been described in more detail in our previous study.[12] Values of the oxide layer thickness derived from the Power-Law formula were between 4 and 5 nm, which is much closer to the thickness of the native titanium oxide layer designated from XPS (8 nm).[45] Moreover, no significant differences were noticed between the oxide layer thickness designated for samples tested in PBS + H_2O_2 and PBS + H_2O_2 + BSA (Table 2).

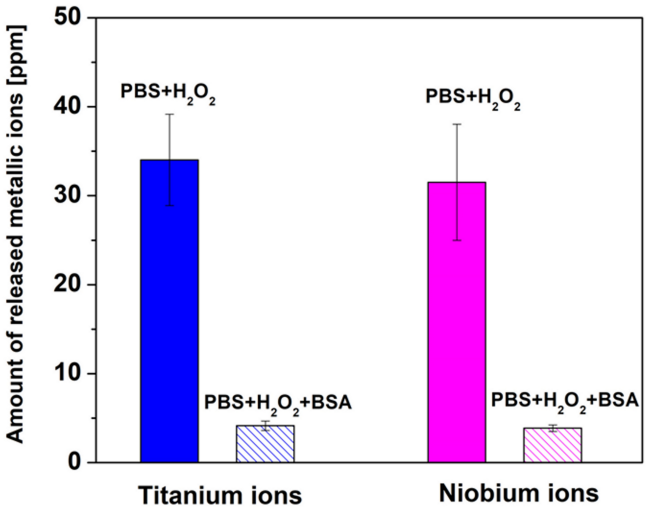

FIGURE 3 Concentrations of Ti and Nb ions released to the PBS + H_2O_2 or PBS + H_2O_2 + BSA after 2 weeks of samples incubation.

$$C_{eff} = Q^{1/n} R_{ox}^{(1-n)/n} \quad (1)$$

$$d_{eff} = \frac{\varepsilon\varepsilon 0}{Ceff} \quad (2)$$

$$C_{eff} = Q(\varepsilon\varepsilon_0\rho_\delta)^{1-n} g \quad (3)$$

$$g = 1 + 2.88(1-n)^{2.375} \quad (4)$$

$$C_{max} = Q(2\pi f_{max})^{n-1} g \quad (5)$$

Long-term corrosion behavior was evaluated based on the calculations of the amount of metal ions released into the PBS + H_2O_2 or

PBS + H_2O_2 + BSA solutions during 2 weeks (336 h) of Ti—Nb immersion (Figure 3). Similarly to the EIS results, ICP-MS tests revealed that albumin suppressed the release of metal ions from the Ti—Nb alloy exposed to the PBS + H_2O_2 ($p < 0.05$). The total concentration of metal ions in PBS + H_2O_2 + BSA was one order of magnitude lower compared to the solution without albumin (Figure 3). The average sum of Ti and Nb ions released into the PBS + H_2O_2 + BSA was ~8 ppm, while for PBS + H_2O_2 was ~65 ppm. Therefore, findings derived from the long-term corrosion analysis are consistent with the conclusions provided based on the EIS tests performed within the initial 24 h of immersion. In order to understand the interaction between albumin and the Ti—Nb surface exposed to the H_2O_2-enriched PBS environment, corrosion measurements were supplemented by post-immersion surface analysis.

Surface chemical composition was analyzed based on the high resolution XPS spectra (Figure 4). In order to gain knowledge about how the surface chemistry is affected by the long-term exposure to simulated inflammatory conditions, XPS measurements were performed before (non-immersed sample) and after 2 weeks of Ti—Nb immersion in the PBS + H_2O_2 or PBS + H_2O_2 + BSA solutions. In the case of the polished, non-immersed sample, metallic Ti and Nb were detected at characteristic binding energies 453.6 and 201.9 eV, respectively (Figure 4A,B). Identification of the peaks originating from the metallic elements implies that the thickness of

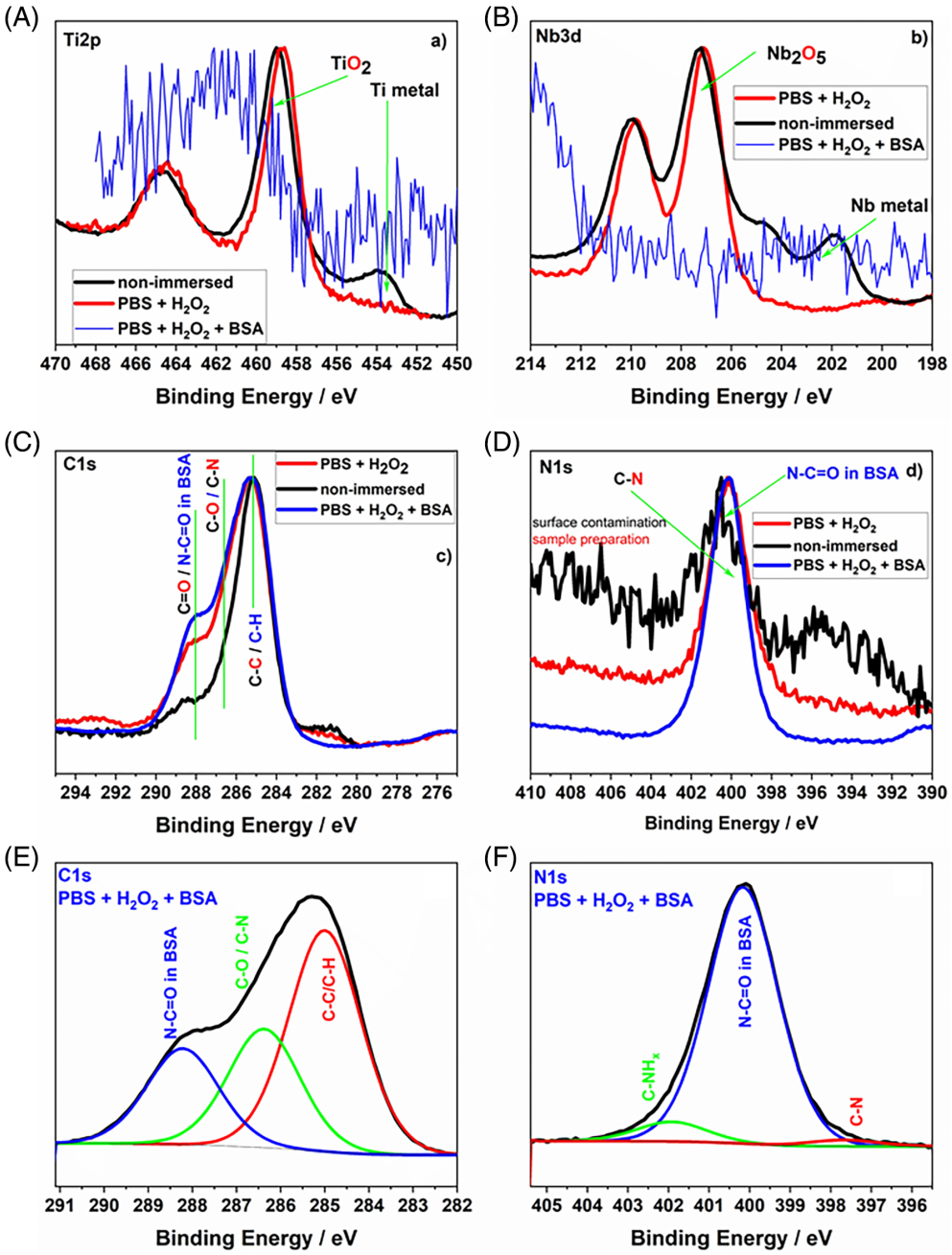

FIGURE 4 XPS spectra that reveal surface chemical composition of Ti—Nb alloy before and after 2 weeks of immersion in PBS + H_2O_2 or PBS + H_2O_2 + BSA: (A–D) immersion-induced evolution of Ti2p, Nb3d, C1s and N1s, respectively, (E) C1s registered in PBS + H_2O_2 + BSA, (F) N1s spectra registered in PBS + H_2O_2 + BSA.

spontaneously-formed passive films did not exceed a few nanometers, which is typical for this type of sample.[46,47] Moreover, detailed XPS studies (data not shown) revealed the presence of following Ti and Nb oxides: TiO_2 (458.9 eV), Ti_2O_3 (457.0 eV), TiO (455.1 eV), Nb_2O_5 (207.2 eV), NbO_2 (205.5 eV), NbO (203.6 eV).[34,46,47] The formation of the oxide layer, which comprises a mixture of oxides with various oxidation states aligns with the model of the air-formed passive film presented by Brunette et al.[35] In our case the dominant signals are peaks assigned to Ti^{4+} and Nb^{5+} (see Figure 4A,B). 2 weeks of immersion in the PBS + H_2O_2 provided substantial changes in the Ti—Nb surface chemical composition. Contrary to the as-polished sample, after the deconvolution procedure, peaks originating from metallic elements and from Ti and Nb oxides on lower oxidation states (Ti_2O_3, TiO, NbO_2, NbO) were not detected (data not shown). The oxidation process of the Ti—Nb alloy under such conditions led to a change in the shape of the Ti2p and Nb3d peaks, which is determined by the presence only the TiO_2 and Nb_2O_5 oxides on the surface (Figure 4A,B). This is related to the growth of the thick oxide layer during prolonged exposure to the PBS + H_2O_2. Similar findings were presented for commercially pure titanium by Tengvall et al.[11] who analyzed H_2O_2-induced growth of the oxide by ellipsometry technique. Moreover, an increase in the layer thickness, from the several nanometers up to 50–60 nm, was revealed for the titanium implant retrieved from the human body after 8 years from surgery.[4,48] For the sample immersed in the PBS + H_2O_2 + BSA solution, no signals from Ti and Nb were detected (see Figure 4A,B). Instead, only peaks from non-metallic elements were recorded (Figure 4A–D). The addition of BSA to the solution led to the covering of the oxide surface with a chemically uniform/continuous layer that exceeds a few nanometers. Deconvolution of the C and N peaks revealed the presence of bonds, which are characteristic for albumin: C—C/C—H (285.0 eV), C—O/C—N (286.5 eV) and N—C═O (288.2 and 400.2 eV), Figure 4E,F.[49] Comparing the C1s and N1s spectra after individual immersion processes (Figure 4C,D), it can be seen that their positions in relation to the binding energy (BE) did not change drastically. This is due to the presence of characteristic C, O and N functional groups, where their BE ranges are close to each other.[50] For the non-immersed sample and the sample exposed to the PBS + H_2O_2, C, O and N compounds on the surface are impurities whose presence is related to the contact with the laboratory atmosphere.[35] Changes in the C and N signal after immersion in the PBS + H_2O_2 solution could be related to the more effective adsorption of impurities to the porous surface developed in the H_2O_2-enriched solution. As was previously mentioned, for the sample exposed to the PBS + H_2O_2 + BSA the C1s and N1s signals can mainly be correlated with the presence of albumin.[49] Moreover, observation of the change in the shape of the C1s carbon peak revealed that the maximum broadening intensity at energy ~288.0 eV is increased in the PBS + H_2O_2 + BSA reaching the characteristic position for the N—C═O bond in albumin.[51] In order to support findings derived from spectroscopic methods, additional TEM studies of the surface cross-sections were conducted.

TEM analysis revealed that the thickness of the oxide film after 2 weeks of immersion in PBS + H_2O_2 was ~30 nm (Figure 5). Moreover, based on TEM observations, it was found that the oxide demonstrated a double-layer structure which confirmed the assumptions included in the pioneering works related to the corrosion behavior of standard Ti-based materials in simulated inflammatory conditions. The first part was a continuous and compact oxide layer, which thickness

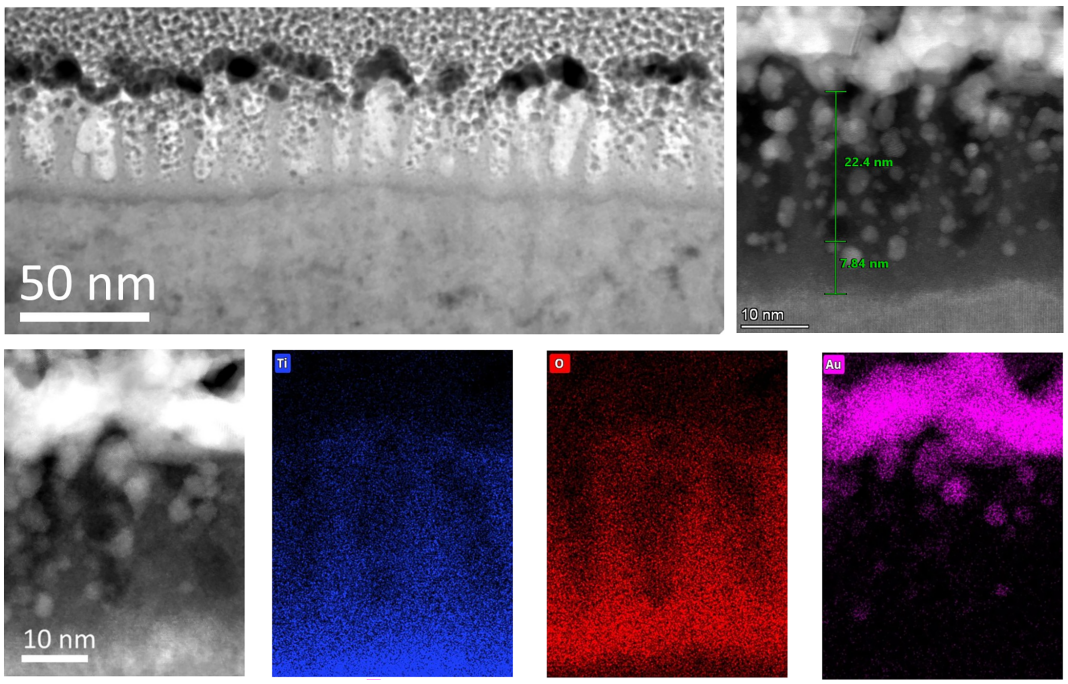

FIGURE 5 TEM and HAADF STEM micrographs of the cross-section Ti—Nb surface after 2-weeks of exposure to the PBS + H_2O_2 and EDS maps of Ti, O and Au distribution, the latter shows distribution of gold particles within the oxide layer.

did not exceed ten nanometers. STEM observations performed with atomic resolution indicated the amorphous character of the compact oxide (Figure 6). The second part of the oxide film was substantially thicker, porous and defective (Figures 5 and 6). Highly porous character of the oxide film is reflected also by discontinuous protective gold layer that was partially sputtered across its thickness, as was indicated by elemental EDS distribution maps (Figure 5).

For the Ti—Nb alloy immersed in the PBS + H_2O_2 + BSA, a continuous layer of adsorbed albumin with a thickness of ~15 nm could be distinguished in the cross-section TEM micrographs (Figure 7), and HAADF STEM micrographs (Figure 7). This confirms the results of post-immersion XPS analysis. Contrary to the surface exposed to the PBS + H_2O_2 solution, the sputtered gold layer was not disrupted, which is related to the smooth character of the albumin film. The oxide film formed in the PBS + H_2O_2 + BSA showed a double-layer structure, similar to that developed in the protein-free solution (Figures 5 and 6). Firstly, a continuous layer, placed in direct vicinity of the bare Ti—Nb alloy, was less than 10 nm in thickness (as in the case of PBS + H_2O_2). However, differences were found in the thickness of defective layers formed in different simulated inflammatory environments (Figures 5 and 7). In the case of PBS + H_2O_2 + BSA, the porous part of the oxide film was substantially thinner (~10 nm) compared to the PBS + H_2O_2 solution (~20–25 nm).

4 | DISCUSSION

Literature data have documented that the significant difference in stiffness between bone tissue and orthopedic implants could prevent the transfer of mechanical stresses from the material to human bone. This phenomenon could result in the bone resorption around the implant and, in the worst cases, lead to implant loosening.[52] Biomedical Ti—Nb alloys respond to this problem by offering remarkably lower elastic modulus values than currently used standard metal-based biomaterials. For several years, research on Ti—Nb alloys has been focused on obtaining a satisfactory balance between elastic modulus and mechanical strength.[53–57] Less attention has been paid to corrosion resistance, which up to date has been characterized in detail mainly in the standard biomedical solutions, which do not sufficiently reflect the complexity of peri-implant fluids.[56,58,59] This study focuses on the analysis of how organic compounds of human fluids (proteins) affect the corrosion behavior of Ti—Nb alloy under simulated inflammatory conditions, which are clinically relevant during the post-operative period.[34] The effect of proteins was simulated by the addition of albumin owing to the fact that it occurs in large concentrations in human fluids, and adsorbs quickly (from seconds to hours) onto the surfaces of biomaterials after their implantation.[60] In order to obtain knowledge about the time-dependent influence of albumin, corrosion behavior was analyzed after short (2 and 24 h) and longer immersion periods (336 h – 2 weeks). Corrosion tests were supplemented by top-view and cross-section analysis, which provided information about the interaction between the metallic surfaces and simulated body fluids. Overall results revealed that albumin significantly enhanced Ti—Nb corrosion resistance under simulated inflammatory conditions.

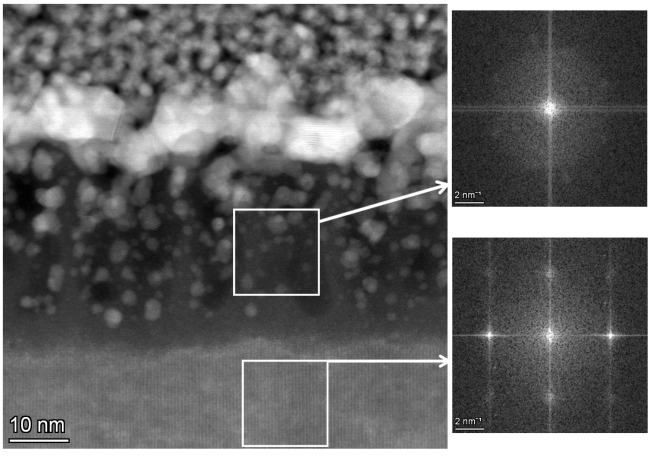

FIGURE 6 HAADF STEM micrograph of the cross-section Ti—Nb surface after 2-weeks of exposure to the PBS + H_2O_2. Fast Fourier transformation (FFT) reflect the crystalline and amorphous structure of Ti—Nb substrate and oxide layer, respectively.

Literature data show that albumin usually slightly enhances or has virtually no effect on the corrosion resistance of Ti-based biomedical alloys. Short-term EIS tests revealed that the presence of albumin in the PBS solution increased the resistance of the passive layer formed on the Ti—6Al—4V surface.[37] On the other hand, virtually no effect of albumin was found based on the results of immersion tests conducted for the long term (22 weeks).[61] Albumin quickly adsorbs onto the metallic surface and reduces the corrosion process by acting as an organic barrier layer in short exposure periods.[24] However, albumin has the ability to create metal-protein complex compounds which could weaken the strength of metal-oxide bonds.[60] Consequently, metal-protein complexes can detach from the surface, and this process can be additionally facilitated by the Vroman effect. This phenomenon is related to the exchange and replacement of the proteins that are bound to the metal/oxide surface.[62] Detachment of albumin-metal complexes from the alloy surface could hinder the slight favorable effect of proteins on its corrosion resistance. Other findings were reported for Ti—6Al—4V exposed to the simulated inflammatory environment. The deleterious effect of albumin on Ti—6Al—4V corrosion resistance under simulated inflammation is believed to be associated with the inhibitory effect of albumin on the cathodic reaction (oxygen reduction), which accelerates the H_2O_2-induced corrosion of Ti. Inhibition of the cathodic reaction was reflected by a lower OCP value (for about 300 mV) registered in the case of Ti—6Al—4V immersed in the PBS + 0.1% H_2O_2 + 4% BSA compared to the PBS + 0.1% H_2O_2.[20] Both potentiodynamic and ICP-MS tests revealed that albumin has a negative impact on Ti—6Al—4V corrosion resistance in PBS + H_2O_2, which is more pronounced in the case of higher proteins concentrations.[20,23] Moreover, EIS tests indicated that the negative influence of albumin is visible mostly in the case of longer immersion periods (>24 h).[22]

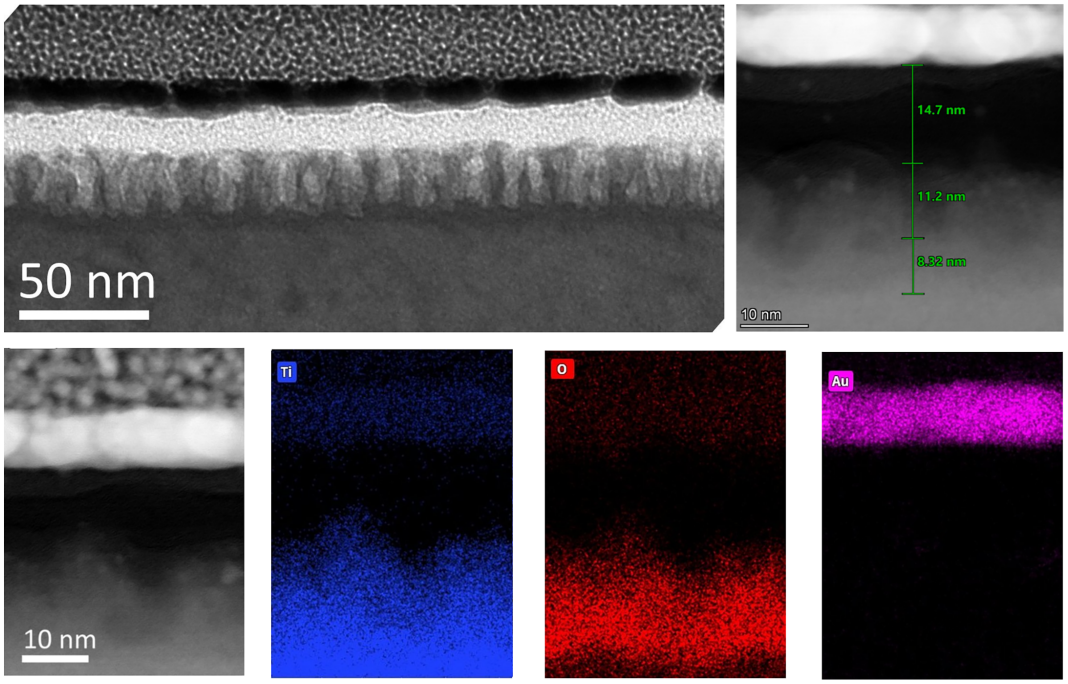

FIGURE 7 TEM and HAADF STEM micrographs of the cross-section Ti—Nb surface after 2-weeks of exposure to the PBS + H_2O_2 + BSA and EDS maps of Ti, O, Au distribution.

Described observations are contradictory to our findings derived from the EIS and ICP-MS data obtained for Ti—Nb tested in two simulated inflammatory solutions (PBS + 0.1% H_2O_2 and PBS + 0.1% H_2O_2 + 4% BSA). According to the short-term EIS tests (2 and 24 h), the oxide layer resistance was an order of magnitude higher in the case of Ti—Nb exposed to the protein-rich solution (Figure 2C). Similarly, the total amount of metal ions detected in the PBS + H_2O_2 + BSA after 2 weeks of immersion, did not exceed a few ppm, while in the PBS + H_2O_2 solution, tens of ppm were detected (Figure 3). Thereby, the results obtained by complementary electrochemical and spectrometric techniques confirmed that albumin influences beneficially the initial as well as prolong corrosion behavior of Ti—Nb under simulated inflammatory conditions. Differences in the corrosion response are strongly related to the surface characteristics tailored by the interaction between Ti—Nb surface and H_2O_2 or H_2O_2 and albumin (Figures 4, 5, 6, and 7). TEM observations revealed the presence of a few nm in thickness compact oxide film on the Ti—Nb surfaces (Figures 5 and 7). Virtually no differences were found in the compact oxide layer thickness observed after immersion in PBS + H_2O_2 and PBS + H_2O_2 + BSA. These results are in agreement with the findings obtained from the calculation of the oxide layer thickness based on capacitance values derived from EIS data using the Power-Law approach (Table 2). The compact oxide layer is responsible for corrosion protection. Generally, the interaction between H_2O_2 and Ti alloys surfaces leads to their dissolution and further deposition in the form of porous and defective oxides.[10,63] In PBS + H_2O_2, the transport of ions across the oxide is facilitated compared to the albumin-rich solution, which resulted in greater dissolution and subsequent pronounced repassivation. It can be noticed that the thickness of the repassivated oxide is around two times greater in the PBS + H_2O_2 compared to those visible after exposure to the PBS + H_2O_2 + BSA solution (Figures 5 and 7). It can be noticed that for Ti—Nb immersed in protein-rich solution, discontinuities within the oxide film were filled with the adsorbed albumin which formed a continuous film on the top of the Ti—Nb surface (Figure 7). Full coverage of the oxide by the organic layer was confirmed by both XPS analysis and TEM observations. Protein could act as a barrier layer against Ti—Nb oxidation induced by H_2O_2. Albumin-limited interaction between Ti and H_2O_2, resulted in suppressing Ti and Nb oxidation, which was reflected by a greater resistance of the oxide layer, lower amount of metal ions detected in the PBS + H_2O_2 + BSA solution, and consequently a thinner layer of the re-deposited oxidation products. Summing up, our study showed that albumin did not decrease the corrosion resistance of the single β-phase Ti—Nb alloy, despite the fact that it was found in literature to accelerate Ti corrosion within the β-phase in case of Ti—6Al—4V (α + β). We believe that the deleterious, synergistic effect of H_2O_2 and albumin on the corrosion behavior of Ti—6Al—4V is related rather to the presence of Al and V. Preferential binding of albumin to Al is accelerated in the case of the defective, H_2O_2-attacked oxide layer. Moreover, the formation and detachment of Al-BSA complexes facilitate Ti oxidation within the β-phase of Ti—6Al—4V.[23]

To the best of the authors' knowledge, this study presents the first attempt to describe the corrosion resistance of the extensively studied group of biomedical Ti—Nb alloys in the complex simulated inflammatory environment that includes the presence of organic compounds found in human blood. Therefore, additional experiments are necessary to fully describe and understand this effect. The process of

early stage albumin adsorption on Ti—Nb surface should be evaluated and compared with Ti—6Al—4V using local combined electrochemical-microscopic techniques such as scanning Kelvin probe force microscopy.[64] This would allow to gain knowledge about the interaction between proteins and the Ti—Nb surface in the presence of H_2O_2 and could provide direct information about the differences in surface behavior between Ti—Nb and Ti—6Al—4V in a protein-rich simulated inflammatory environment. Future work should also consider the effect of microstructure on Ti—Nb corrosion behavior in PBS + H_2O_2 + albumin, which could be refined in order to alter alloy's mechanical properties.[54,55] Moreover, similar corrosion evaluation should also be repeated for other promising Ti β-phase biomedical alloys that contain different β-phase stabilizers.

5 | CONCLUSIONS

In this work, the effect of albumin on the corrosion resistance of biomedical β-phase Ti—Nb alloy was investigated in the PBS + H_2O_2 fluid, which simulates the conditions created by immune cells in the post-operative inflammation period. The main conclusions derived from this study are as follows:

- Albumin significantly enhances the corrosion resistance of Ti—Nb alloy under simulated inflammatory conditions. This was confirmed by the higher values of oxide layer resistances designated from the EIS tests performed after 2 and 24 h of immersion in the albumin-rich solution ($R_{ox} = 0.03–0.04\ M\Omega \times cm^2$ in PBS + H_2O_2 and $R_{ox} \approx 0.13–0.20\ M\Omega \times cm^2$ in PBS + H_2O_2 + BSA) and by the lower concentration of metal ions detected after 2 weeks of exposure (~65 ppm in PBS + H_2O_2 and ~8 ppm in PBS + H_2O_2 + BSA). Therefore, the beneficial effect of albumin was visible in both short and long-term of Ti—Nb exposure to the tested solutions.
- Two weeks of Ti—Nb exposure in the PBS + H_2O_2 + BSA solution resulted in complete surface coverage by the adsorbed albumin. This was confirmed by both analysis of the surface chemical composition (XPS) and observations of the surface cross-sections (TEM and STEM). The thickness of the albumin layer was ~15 nm.
- Adsorption of albumin suppresses Ti—Nb oxidation induced by H_2O_2 and further growth of the defective oxide layer. The overall thickness of the oxide film formed in the PBS + H_2O_2 was ~30 nm, while in the PBS + H_2O_2 + BSA, it did not exceed 20 nm.
- Contrary to Ti—6Al—4V (α + β), an undesirable synergistic effect of albumin and H_2O_2 on the corrosion resistance was not observed for Ti—Nb (β). Results of the short and long-term corrosion studies indicate that the addition of blood/serum proteins to the physiological solutions is not necessary to simulate the harsh inflammatory environment.

ACKNOWLEDGMENTS

This research was supported financially by the National Science Centre, Poland under the grant PRELUDIUM 15 [2018/29/N/ST8/02306]. National Science Centre financed EIS, ICP-MS, XPS, TEM, HAADF STEM studies. FIB preparation was funded through the European Union Horizon 2020 research and innovation program under Grant Agreement No. 857470 and from the European Regional Development Fund of the Foundation for Polish Science International Research Agenda PLUS program Grant No. MAB PLUS/2018/8 and the initiative of the Ministry of Science and Higher Education 'Support for the activities of Centers of Excellence established in Poland under the Horizon 2020 program' under agreement No. MEiN/2023/DIR/3795. We are grateful to Mrs. Agnieszka Kamińska for her support in the preparation of protein-contained solutions for the ICP-MS tests.

CONFLICT OF INTEREST STATEMENT

The authors declare no conflicts of interest.

DATA AVAILABILITY STATEMENT

The data that support the findings of this study are available from the corresponding author upon reasonable request.

ORCID

Agata Sotniczuk https://orcid.org/0000-0002-3468-0468

REFERENCES

1. Chen L-Y, Zhang H-Y, Zheng C, et al. Corrosion behavior and characteristics of passive films of laser powder bed fusion produced Ti–6Al–4V in dynamic Hank's solution. *Mater Des*. Elsevier. 2021;208:109907.
2. ASTM F1801-97. *Standard Practice for Corrosion Fatigue Testing of Metallic Implant Materials*. ASTM International; 2014.
3. ASTM F2129. Standard Test Method for Conducting Cyclic Potentiodynamic Polarization Measurements to Determine the Corrosion Susceptibility of Small Implant Devices.
4. Prestat M, Thierry D. Corrosion of titanium under simulated inflammation conditions: clinical context and in vitro investigations. *Acta Biomater* Elsevier. 2021;136:72-87.
5. Gilbert JL, Sivan S, Liu Y, Kocagöz SB, Arnholt CM, Kurtz SM. Direct in vivo inflammatory cell-induced corrosion of CoCrMo alloy orthopedic implant surfaces. *J Biomed Mater Res Part A*. Wiley Online Library. 2015;103:211-223.
6. Gilbert JL. Corrosion in the human body: metallic implants in the complex body environment. *Corros Nat Assoc Corros Eng Int*. 2017;73:1478-1495.
7. Kubacki GW, Gilbert JL. The effect of the inflammatory species hypochlorous acid on the corrosion and surface damage of Ti–6Al–4V and CoCrMo alloys. *J Biomed Mater Res Part A*. Wiley Online Library. 2018;106:3185-3194.
8. Zhang Y, Davenport AJ, Burke B, Vyas N, Addison O. Effect of Zr addition on the corrosion of Ti in acidic and reactive oxygen species (ROS)-containing environments. *ACS Biomater Sci Eng* ACS Publications. 2018;4:1103-1111.
9. Kurtz MA, Wessinger AC, Mace A, Moreno-Reyes A, Gilbert JL. Additively manufactured Ti–29Nb–21Zr shows improved oxide polarization resistance versus Ti–6Al–4V in inflammatory simulating solution. *J Biomed Mater Res Part A*. Wiley Online Library. 2023;111(10):1538-1553.
10. Pan J, Thierry D, Leygraf C. Electrochemical and XPS studies of titanium for biomaterial applications with respect to the effect of hydrogen peroxide. *J Biomed Mater Res*. Wiley Online Library. 1994;28:113-122.

11. Tengvall P, Lundström I, Sjöqvist L, Elwing H, Bjursten LM. Titanium-hydrogen peroxide interaction: model studies of the influence of the inflammatory response on titanium implants. *Biomaterials* Elsevier. 1989;10:166-175.
12. Sotniczuk A, Chromiński W, Adamczyk-Cieślak B, Pisarek M, Garbacz H. Corrosion behaviour of biomedical Ti under simulated inflammation: exploring the relevance of grain refinement and crystallographic texture. *Corros Sci*. Elsevier. 2022;200:110238.
13. Kurtz MA, Khullar P, Gilbert JL. Cathodic activation and inflammatory species are critical to simulating in vivo Ti–6Al–4V selective dissolution. *Acta Biomater* Elsevier. 2022;149:399-409.
14. Prestat M, Vucko F, Holzer L, Thierry D. Microstructural aspects of Ti6Al4V degradation in H_2O_2-containing phosphate buffered saline. *Corros Sci*. Elsevier. 2021;190:109640.
15. Bearinger JP, Orme CA, Gilbert JL. Effect of hydrogen peroxide on titanium surfaces: in situ imaging and step-polarization impedance spectroscopy of commercially pure titanium and titanium, 6-aluminum, 4-vanadium. *J Biomed Mater Res Part A Off J Soc Biomater Jpn Soc Biomater Aust Soc Biomater Korean Soc Biomater*. Wiley Online Library. 2003;67:702-712.
16. Fonseca C, Barbosa M. Corrosion behaviour of titanium in biofluids containing H_2O_2 studied by electrochemical impedance spectroscopy. *Corros Sci*. 2001;43:547-559.
17. Pan J, Thierry D, Leygraf C. Electrochemical impedance spectroscopy study of the passive oxide film on titanium for implant application. *Electrochim Acta*. Elsevier. 1996;41:1143-1153.
18. Fonseca-García A, Pérez-Alvarez J, Barrera CC, et al. The effect of simulated inflammatory conditions on the surface properties of titanium and stainless steel and their importance as biomaterials. *Mater Sci Eng C*. 2016;66:119-129.
19. Spriano S, Yamaguchi S, Baino F, Ferraris S. A critical review of multifunctional titanium surfaces: new frontiers for improving osseointegration and host response, avoiding bacteria contamination. *Acta Biomater*. Elsevier. 2018;79:1-22.
20. Yu F, Addison O, Davenport AJ. A synergistic effect of albumin and H_2O_2 accelerates corrosion of Ti6Al4V. *Acta Biomater*. 2015;26:355-365.
21. Gopal V, Manivasagam G. Wear – Corrosion synergistic effect on Ti–6Al–4V alloy in H_2O_2 and albumin environment. *J Alloys Compd*. Elsevier. 2020;830:154539.
22. Zhang Y, Addison O, Yu F, Troconis BCR, Scully JR, Davenport AJ. Time-dependent enhanced corrosion of Ti6Al4V in the presence of H_2O_2 and albumin. *Sci Rep*. Nature Publishing Group. 2018;8:3185.
23. Hedberg YS, Žnidaršič M, Herting G, Milošev I, Odnevall WI. Mechanistic insight on the combined effect of albumin and hydrogen peroxide on surface oxide composition and extent of metal release from Ti6Al4V. *J Biomed Mater Res Part B Appl Biomater*. Wiley Online Library. 2019;107:858-867.
24. Hedberg YS, Gamna F, Padoan G, et al. Surface modified Ti6Al4V for enhanced bone bonding ability–effects of silver and corrosivity at simulated physiological conditions from a corrosion and metal release perspective. *Corros Sci*. Elsevier. 2020;168:108566.
25. Rahimi E, Offoiach R, Baert K, Terryn H, Lekka M, Fedrizzi L. Role of phosphate, calcium species and hydrogen peroxide on albumin protein adsorption on surface oxide of Ti6Al4V alloy. *Materialia* Elsevier. 2021;15:100988.
26. Alberta LA, Vishnu J, Hariharan A, Pilz S, Gebert A, Calin M. Novel low modulus beta-type Ti–Nb alloys by gallium and copper minor additions for antibacterial implant applications. *J Mater Res Technol*. Elsevier. 2022;20:3306-3322.
27. Pilz S, Hariharan A, Günther F, Zimmermann M, Gebert A. Influence of isothermal omega precipitation aging on deformation mechanisms and mechanical properties of a β-type Ti-Nb alloy. *J Alloys Compd*. Elsevier. 2023;930:167309.
28. Çaha I, Alves AC, Chirico C, et al. Atomic–scale investigations of passive film formation on Ti-Nb alloys. *Appl Surf Sci*. Elsevier. 2023;615:156282.
29. Pilz S, Gustmann T, Günther F, Zimmermann M, Kühn U, Gebert A. Controlling the Young's modulus of a ß-type Ti-Nb alloy via strong texturing by LPBF. *Mater Des* Elsevier. 2022;216:110516.
30. Roshchina MY, Querebillo CJ, Dmitrieva E, et al. Corrosion behavior of an oxide nanotube-coated β-type Ti–45Nb implant alloy in a simulated inflammatory solution. *Corros Sci*. Elsevier. 2024;227:111767.
31. Gostin PF, Helth A, Voss A, et al. Surface treatment, corrosion behavior, and apatite-forming ability of Ti–45Nb implant alloy. *J Biomed Mater Res Part B Appl Biomater*. Wiley Online Library. 2013;101:269-278.
32. Caha I, Alves AC, Kuroda PAB, et al. Degradation behavior of Ti-Nb alloys: corrosion behavior through 21 days of immersion and tribocorrosion behavior against alumina. *Corros Sci*. Elsevier. 2020;167:108488.
33. Bai Y, Deng Y, Zheng Y, et al. Characterization, corrosion behavior, cellular response and in vivo bone tissue compatibility of titanium–niobium alloy with low Young's modulus. *Mater Sci Eng C* Elsevier. 2016;59:565-576.
34. Sotniczuk A, Gilbert JL, Liu Y, et al. Corrosion resistance of β-phase titanium alloys under simulated inflammatory conditions: exploring the relevance of biocompatible alloying elements. *Corros Sci* Elsevier. 2023;220:111271.
35. Brunette DM, Tengvall P, Textor M, Thomsen P. *Titanium in Medicine: Material Science, Surface Science, Engineering, Biological Responses and Medical Applications*. Springer Science & Business Media; 2012.
36. Cheng X, Roscoe SG. Corrosion behavior of titanium in the presence of calcium phosphate and serum proteins. *Biomaterials*. 2005;26:7350-7356.
37. Karimi S, Nickchi T, Alfantazi A. Effects of bovine serum albumin on the corrosion behaviour of AISI 316L, Co–28Cr–6Mo, and Ti–6Al–4V alloys in phosphate buffered saline solutions. *Corros Sci Pergamon*. 2011;53:3262-3272.
38. Della Rovere CA, Alano JH, Silva R, Nascente PAP, Otubo J, Kuri SE. Characterization of passive films on shape memory stainless steels. *Corros Sci*. Elsevier. 2012;57:154-161.
39. Orazem ME, Frateur I, Tribollet B, et al. Dielectric properties of materials showing constant-phase-element (CPE) impedance response. *J Electrochem Soc* IOP Publishing. 2013;160:C215-C225.
40. Hirschorn B, Orazem ME, Tribollet B, Vivier V, Frateur I, Musiani M. Determination of effective capacitance and film thickness from constant-phase-element parameters. *Electrochim Acta* Elsevier. 2010;55:6218-6227.
41. Hamadou L, Aïnouche L, Kadri A, Yahia SAA, Benbrahim N. Electrochemical impedance spectroscopy study of thermally grown oxides exhibiting constant phase element behaviour. *Electrochim Acta*. Elsevier. 2013;113:99-108.
42. Kubacka D, Yamamoto A, Wieciński P, Garbacz H. Biological behavior of titanium processed by severe plastic deformation. *Appl Surf Sci*. 2019;472:54-63.
43. Garbacz H, Pisarek M, Kurzydłowski KJ. Corrosion resistance of nanostructured titanium. *Biomol Eng* Elsevier. 2007;24:559-563.
44. Hirschorn B, Orazem ME, Tribollet B, Vivier V, Frateur I, Musiani M. Constant-phase-element behavior caused by resistivity distributions in films: II. *Appl J Electr Soc* IOP Publishing. 2010;157:C458.
45. McCafferty E, Wightman JP. An X-ray photoelectron spectroscopy sputter profile study of the native air-formed oxide film on titanium. *Appl Surf Sci*. Elsevier. 1999;143:92-100.
46. López MF, Jiménez JA, Gutiérrez A. XPS characterization of surface modified titanium alloys for use as biomaterials. *Vacuum* Elsevier. 2011;85:1076-1079.

47. Yang X, Li X, Liu Z, Du C, Qian W, Li X. Passivity study of titanium alloy TA2 in simulated seawater solution. *J Mater Res Technol* Elsevier. 2023;26:4797-4812.
48. Sundgren JE, Bodö P, Lundström I. Auger electron spectroscopic studies of the interface between human tissue and implants of titanium and stainless steel. *J Colloid Interface Sci* Elsevier. 1986;110:9-20.
49. Cai K, Bossert J, Jandt KD. Does the nanometre scale topography of titanium influence protein adsorption and cell proliferation? *Colloids Surf B Biointerfaces* Elsevier. 2006;49:136-144.
50. Chastain J, King RC Jr. Handbook of X-ray photoelectron spectroscopy. *Perkin-Elmer Corp*. 1992;40:221.
51. Pisarek M, Roguska A, Marcon L, Andrzejczuk M, Janik-Czachor M. Enhanced bioactivity of calcium phosphate coatings obtained by a direct electrodeposition from Hanks' solution on Ti surface. *Arch Metall Mater*; Polska Akademia Nauk. Czytelnia Czasopism PAN. 2013;58:261-267.
52. Nagels J, Stokdijk M, Rozing PM. Stress shielding and bone resorption in shoulder arthroplasty. *J Shoulder Elb Surg* Elsevier. 2003;12:35-39.
53. Helth A, Pilz S, Kirsten T, et al. Effect of thermomechanical processing on the mechanical biofunctionality of a low modulus Ti–40Nb alloy. *J Mech Behav Biomed Mater* Elsevier. 2017;65:137-150.
54. Ozaltin K, Chrominski W, Kulczyk M, et al. Enhancement of mechanical properties of biocompatible Ti–45Nb alloy by hydrostatic extrusion. *J Mater Sci* Springer. 2014;49:6930-6936.
55. Cvijović-Alagić I, Laketić S, Bajat J, Hohenwarter A, Rakin M. Grain refinement effect on the Ti–45Nb alloy electrochemical behavior in simulated physiological solution. *Surf Coat Technol* Elsevier. 2021;423:127609.
56. Hu N, Xie L, Liao Q, et al. A more defective substrate leads to a less defective passive layer: enhancing the mechanical strength, corrosion resistance and anti-inflammatory response of the low-modulus Ti–45Nb alloy by grain refinement. *Acta Biomater*. Elsevier. 2021;126:524-536.
57. Guo S, Zhang J, Cheng X, Zhao X. A metastable β-type Ti–Nb binary alloy with low modulus and high strength. *J Alloys Compd* Elsevier. 2015;644:411-415.
58. Bai YJ, Wang YB, Cheng Y, Deng F, Zheng YF, Wei SC. Comparative study on the corrosion behavior of Ti–Nb and TMA alloys for dental application in various artificial solutions. *Mater Sci Eng C*. Elsevier. 2011;31:702-711.
59. Fojt J, Joska L, Malek J, Sefl V. Corrosion behavior of Ti–39Nb alloy for dentistry. *Mater Sci Eng C*. Elsevier. 2015;56:532-537.
60. Hedberg YS. Role of proteins in the degradation of relatively inert alloys in the human body. *NPJ Mater Degrad*. Nature Publishing Group UK London. 2018;2:26.
61. Karimi S, Nickchi T, Alfantazi AM. Long-term corrosion investigation of AISI 316L, Co–28Cr–6Mo, and Ti–6Al–4V alloys in simulated body solutions. *Appl Surf Sci*. Elsevier. 2012;258:6087-6096.
62. Hirsh SL, McKenzie DR, Nosworthy NJ, Denman JA, Sezerman OU, Bilek MMM. The Vroman effect: competitive protein exchange with dynamic multilayer protein aggregates. *Colloids Surf B Biointerfaces* Elsevier. 2013;103:395-404.
63. Pan J, Thierry D, Leygraf C. Hydrogen peroxide toward enhanced oxide growth on titanium in PBS solution: blue coloration and clinical relevance. *J Biomed Mater Res off J Soc Biomater Jpn Soc Biomater*. Wiley Online Library. 1996;30:393-402.
64. Rahimi E, Offoiach R, Hosseinpour S, et al. Effect of hydrogen peroxide on bovine serum albumin adsorption on Ti6Al4V alloy: a scanning Kelvin probe force microscopy study. *Appl Surf Sci* Elsevier. 2021;563:150364.

How to cite this article: Sotniczuk A, Kalita D, Chromiński W, Matczuk M, Pisarek M, Garbacz H. Albumin suppresses oxidation of Ti—Nb alloy in the simulated inflammatory environment. *J Biomed Mater Res*. 2024;112(4):e35404. doi:10.1002/jbm.b.35404